16.4 Energy-Autonomous Fever Alarm Armband Integrating Fully Flexible Solar Cells, Piezoelectric Speaker, Temperature Detector, and 12V Organic Complementary FET Circuits

Hiroshi Fuketa[1,2], Masamune Hamamatsu[1,2], Tomoyuki Yokota[1,2], Wakako Yukita[1,2], Teruki Someya[1,2], Tsuyoshi Sekitani[2,3], Makoto Takamiya[1,2], Takao Someya[1,2], Takayasu Sakurai[1,2]

[1]University of Tokyo, Tokyo, Japan,
[2]JST/ERATO, Tokyo, Japan,
[3]Osaka University, Osaka, Japan

Three key requirements for wearable healthcare and biomedical devices are the mechanical flexibility, the wireless interface, and the energy autonomy, because unobtrusive and maintenance-free devices are needed for the constant monitoring of vital human health data. Previously reported flexible healthcare and biomedical devices, however, requires wired connection [1,2] or wireless power transmission [3,4]. A flexible energy autonomous healthcare device with a wireless interface, a fever alarm armband (FAA) integrating fully flexible solar cells, a piezoelectric speaker, a temperature detector, and 12V organic complementary FET (CFET) circuits is presented here. The system is also noteworthy for sound generation, with organic circuits driving the speaker.

Figure 16.4.1 shows a photograph of FAA with the size of 30x18cm^2 and its use case. All components in FAA are mechanically flexible. FAA is looped around an upper arm of a patient in a hospital room, and the temperature detector monitors the underarm temperature of the patient. A 220μm thick amorphous silicon solar cells (PowerFilm P3-37) attached outside of the upper arm generate the power (e.g. 3mW at 1500lx). When high fever is detected, a 52μm thick piezoelectric speaker with polyvinylidene difluoride (PVDF) makes a sound to alarm a nurse. Organic CFET circuits and the temperature detector are fabricated on a 50μm thick flexible polyimide film, and the solar cells and the speaker are attached on it.

Figure 16.4.2 shows a circuit schematic of FAA. An active voltage limiter (AVL) regulates the power supply voltage (V_{DD}) of the FAA, because V_{DD} changes depending on both the illuminance for the solar cells and the power consumption of the FAA. When the measured temperature is higher than the preset threshold temperature (T_t), the ring oscillator (RO) starts oscillation and the speaker makes a sound. Two design challenges of the FAA are as follows. 1) In the temperature detector, variable T_t by users is required, because the needed T_t depends on the patient. 2) The voltage regulation of V_{DD} is required, because the output voltage change of the solar cells due to the variation of the indoor lighting is large (e.g. 10V at 500lx and 20V at 3000lx) and the overvoltage breaks down the organic transistors. In the organic electronics, however, the voltage regulation is difficult, because a voltage reference and Zener diodes are not available. To solve these problems, the following two solutions are proposed in this paper. 1) A voltage controlled threshold temperature tuning (VCTTT) enables the tuning of T_t. 2) AVL is the world's first voltage regulation in the organic electronics.

Figures 16.4.3 (a) and (b) show a circuit schematic and the measured temperature dependence of the temperature detector, respectively. When the temperature is increased, the resistance of a resistive-type flexible thermal sensor increases by more than 10^4 times at T_t, and $\overline{EN}$ changes from high to low. In the proposed VCTTT, the gate voltage (V_G) of p-type transistor operating in the sub-threshold region is varied to tune T_t. When V_G is varied from 10V to 12V, T_t changes from 36.5°C to 38.5°C, which indicates 1°C/V tunability. The control of V_G could be achieved by selectively cutting the wires of a resistor ladder, though a V_G generator is not implemented in the FAA.

In the FAA, a careful choice of the frequency of the sound is required, because the frequency is determined by both RO and the speaker. Figure 16.4.4(a) shows the measured V_{DD} dependence of the RO frequency. The maximum frequency of RO is 6kHz, because the maximum V_{DD} (V_{MAX}) is 15V due to the breakdown voltage of the transistors. In contrast, the speaker does not make a sound below 1.8kHz. Therefore, the target frequency of the sound is selected to be 4.7kHz, because the speaker itself has the maximum sound pressure level (SPL) at 5kHz within a range of 1.8kHz to 6kHz. The corresponding target V_{DD} for RO is 12V. Figure 16.4.4 (a) also shows V_{DD} dependence of SPL of the speaker at RO frequency measured with a sound level meter (RION NL-32) at 30cm distance. The minimum V_{DD} (V_{MIN}) is defined as 9V at SPL of 10dB corresponding to the background noise. Figure 16.4.4(b) shows the measured waveform of the input signal of the speaker ("Out" in Fig. 16.4.2) at 12V and 4.7kHz. The power consumption of RO and the driver is 2.2mW. Figures 16.4.4 (c) and (d) show the measured spectra of SPL without and with the speaker, respectively. Figure 16.4.4(c) shows background noise in the measurement room. As shown in Fig. 16.4.4(d), the speaker successfully makes a sound with SPL of 28dB at 4.7kHz and the SNR is 18dB.

Figures 16.4.5(a) and (b) show circuit schematics of the proposed AVL and a conventional diode clamp for comparison, respectively. AVL is a kind of a shunt regulator, and is composed of a constant voltage generator, two CFET inverters, and a power transistor (M5). The constant voltage (V_1) and a logical threshold voltage of the inverter (~V_{DD}/2) are compared, and the output of the inverter (V_2) is varied to regulate V_{DD}. The essence of the constant voltage generator is stacked diode-connected transistor (M1) with small W/L and OFF transistor (M2) with large W/L. When the channel length modulation effect of the transistors is neglected, V_3 is constant without a dependence on V_{DD}, because M2 is a constant current source with the OFF current and V_{DS} (=V_{GS}) of M1 is determined by the OFF current. To increase the constant voltage V_3 to V_{DD}/2 (=6V), M3 and M4 are added, and V_1=2xV_3. Figure 16.4.5(c) shows the measured V_{DD} dependence of V_1 and V_2 in AVL. When V_{DD} is within 7V to 15V, V_1 stays around 6.5V and $\Delta V_1/\Delta V_{DD}$=6% due to the channel length modulation. Figure 16.4.5(d) shows the measured V_{DD} dependence of I_D of AVL and the conventional diode clamp. In Fig. 16.4.5(d), the maximum $\Delta I_D/\Delta V_{DD}$ of the diode clamp and AVL is 63μA/V and 121μA/V, respectively, which indicates that AVL increases $\Delta I_D/\Delta V_{DD}$ by 1.9 times.

The impact of AVL on the operational illuminance range of FAA is shown. Figures 16.4.6(a), (b) and (c) show the measured illuminance dependence of V_{DD} without the voltage limiter, with the conventional diode clamp, and with the proposed AVL, respectively. Two lines in each figure show with and without activating the load circuits (RO and the driver) in Fig. 16.4.2. The maximum and minimum operational illuminance are determined by V_{MAX} (=15V) and V_{MIN} (=9V), respectively. Without the voltage limiter in Fig. 16.4.6(a), the operational illuminance range is 300lx. By adding the conventional diode clamp in Fig. 16.4.6(b), the range is 1900lx. In the proposed AVL in Fig. 16.4.6(c), the range is 2200lx. AVL simultaneously achieves the minimum illuminance of Fig. 16.4.6(a) and the maximum illuminance of Fig. 16.4.6(b) thanks to the sharp I_D control shown in Fig. 16.4.5(d). Thus, AVL increases the operational illuminance range from 300lx to 2200lx by 7.3 times.

Figure 16.4.7 shows micrographs of the organic circuits and a summary of the organic CFET. The organic semiconductors for p-type and n-type transistors are DNTT [4] and PDI-8CN2 [5], respectively. The minimum gate length is 10μm.

Acknowledgment:
The authors thank Dr. Zhouyu Ji of Institute of Microelectronics of Chinese Academy of Sciences for valuable discussion.

References:
[1] J. Viventi, *et al.,* "Flexible, Foldable, Actively Multiplexed, High-Density Electrode Array for Mapping Brain Activity in Vivo," *Nature Neurosciences*, vol. 14, pp. 1599–1605, Dec. 2011.
[2] H. Fuketa, *et al.,* "1μm-Thickness 64-Channel Surface Electromyogram Measurement Sheet with 2V Organic Transistors for Prosthetic Hand Control," *ISSCC Dig. of Tech. Papers*, pp. 104-105, Feb. 2013.
[3] D.H. Kim, *et al.,* "Epidermal Electronics," *Science*, vol. 333, pp. 838-843, Aug. 2011.
[4] H. Fuketa, *et al., "*Organic Transistor Based 2kV ESD Tolerant Flexible Wet Sensor Sheet for Biomedical Applications with Wireless Power and Data Transmission Using 13.56MHz Magnetic Resonance," *ISSCC Dig. of Tech. Papers*, pp. 490-491, Feb. 2014.
[5] L. Li, *et al.,"*High-Performance and Stable Organic Transistors and Circuits with Patterned Polypyrrole Electrodes," *Advanced Materials*, vol. 24, pp. 2159-2164, Apr. 2012.

 978-1-4799-6224-2/15/$31.00 ©2015 IEEE

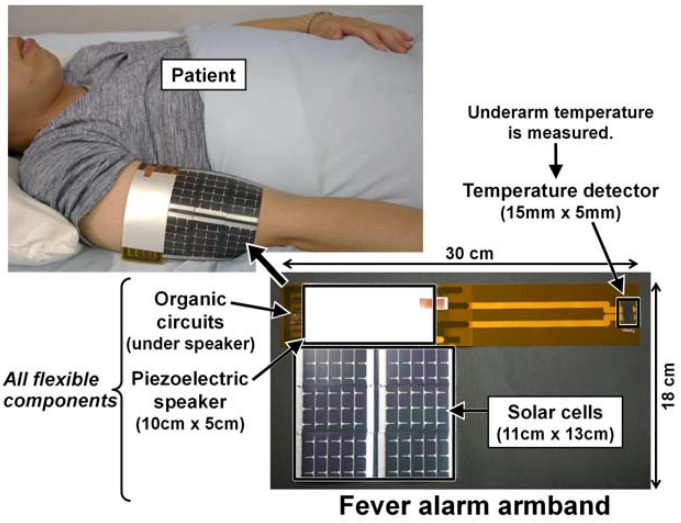

Figure 16.4.1: Developed fever alarm armband.

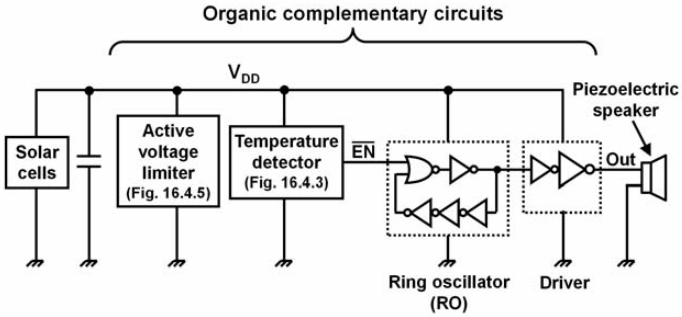

Figure 16.4.2: Circuit schematic of fever alarm armband.

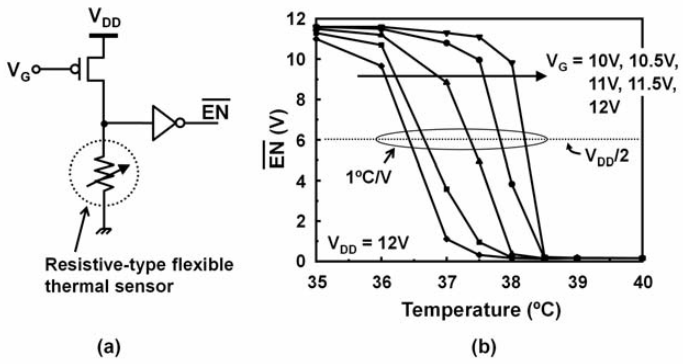

Figure 16.4.3: Temperature detector. (a) Circuit schematic. (b) Measured temperature dependence of output voltage with proposed voltage controlled threshold temperature tuning (VCTTT).

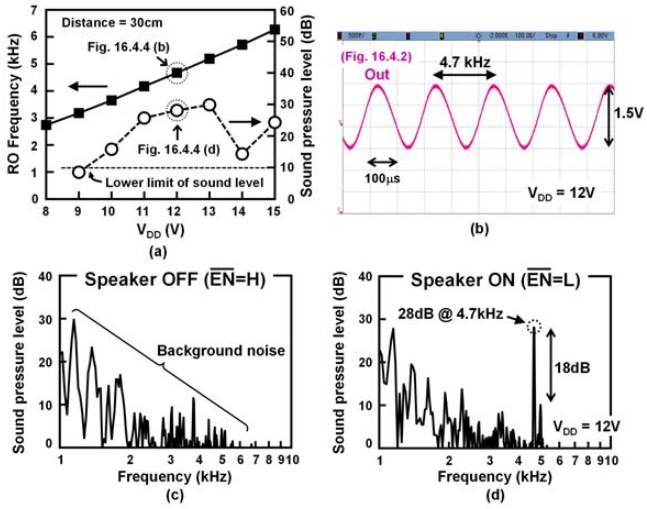

Figure 16.4.4: Circuits to make sound. (a) Measured V_{DD} dependence of RO frequency and sound pressure level. (b) Measured waveform of Out in Fig. 16.4.2. (c) & (d) Measured spectra of sound pressure level.

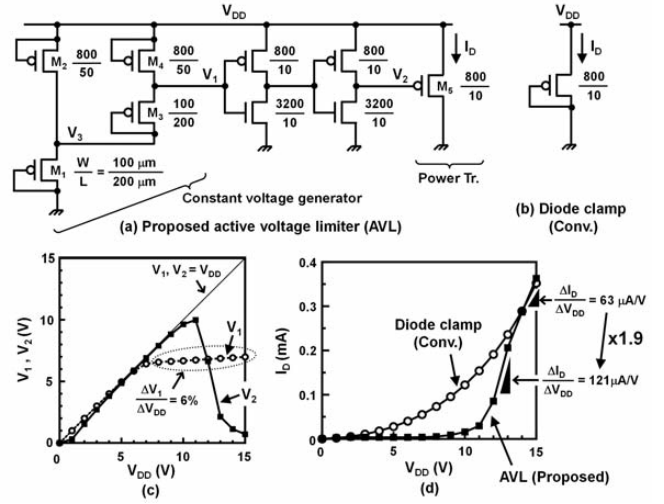

Figure 16.4.5: (a) Proposed active voltage limiter (AVL). (b) Conventional diode clamp. (c) Measured V_{DD} dependence of V_1 and V_2 in AVL. (d) Measured V_{DD} dependence of I_D.

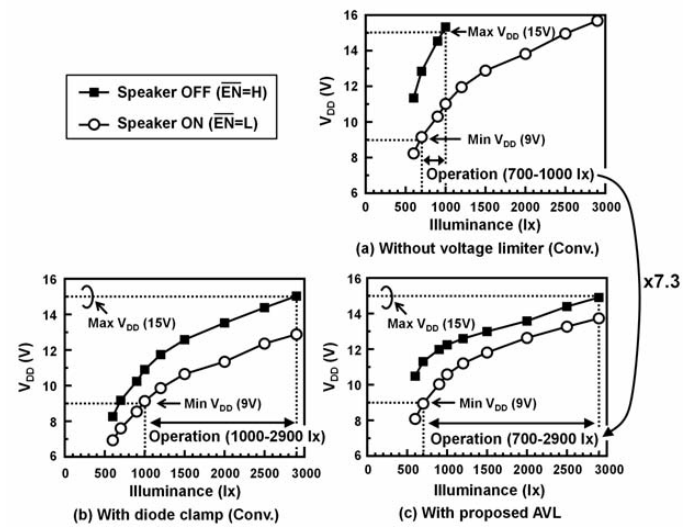

Figure 16.4.6: Measured illuminance dependence of V_{DD}, (a) without voltage limiter, (b) with conventional diode clamp, and (c) with proposed AVL.

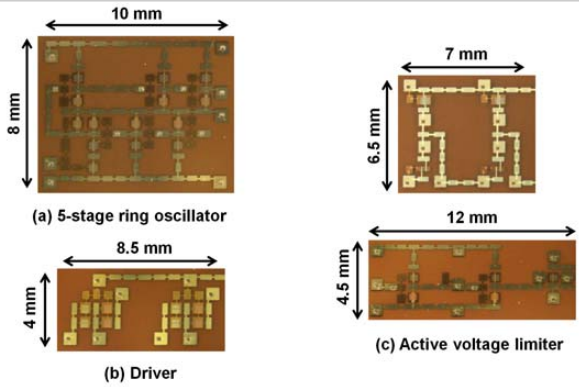

Organic complementary transistors		
Semiconductor material	P-type	DNTT (μ = 1.0 cm^2/Vs)
	N-type	PDI-8CN2 (μ = 0.05 cm^2/Vs)
Gate insulator, thickness	Parylene (40-50nm thick)	
Minimum gate length	10 µm	

Figure 16.4.7: Micrographs of organic circuits and summary of organic CFET.

978-1-4799-6224-2/15/$31.00 ©2015 IEEE